Physiologia Plantarum

ORIGINAL RESEARCH OPEN ACCESS

Non-Vessel Water Flow in Angiosperm Trees Enables Bypassing of Partially Blocked Xylem

Yannik Müllers[1] | Uri Hochberg[2] | Guy Perri[1] | Tamir Klein[1]

[1]Weizmann Tree Lab, Department of Plant & Environmental Sciences, Weizmann Institute of Science, Rehovot, Israel | [2]Agricultural Research Organization, Volcani Center, Institute of Soil, Water and Environmental Sciences, Neve Ya'ar Research Station, Ramat Yishai, Israel

Correspondence: Yannik Müllers (yannik.muellers@weizmann.ac.il)

Received: 29 November 2025 | **Revised:** 30 January 2026 | **Accepted:** 2 February 2026

Handling Editor: K. Noguchi

Keywords: hydraulic bypassing | leaf water supply | stem notching | vessel blockage | xylem embolism

ABSTRACT

Blockage of xylem vessels can compromise water flow in trees, eventually leading to reduced gas exchange and productivity. The extent of these impairments also depends on how effectively blocked vessels can be bypassed through lateral pathways. We hypothesize that the ability to bypass can vary crucially between different species of the same clade, leading to differences in the hydraulic limitations after a defined loss of conducting vessels. Here, we test this hypothesis on 1-year-old seedlings of two Mediterranean angiosperm tree species, carob (*Ceratonia siliqua*) and oak (*Quercus calliprinos*). We consecutively notched stems to artificially block water flow through vessels in one half of the cross-section. We measured the effect of notching on leaf gas exchange and visualized altered water flow pathways using microscopy and μCT imaging. In carobs, stomatal conductance (g_s) of leaves on the notched side decreased by more than 90%. Water transport in the notched side of the stem had ceased. In oaks, leaves on the notched side maintained more than 50% of their g_s with no signs of dehydration. Microscopy and μCT imaging revealed that water supply to these leaves occurred through lateral pathways outside vessels. This can be explained by the presence of tangentially oriented arrays of tracheids with bordered pits, which we found in oaks but not carobs. Our study emphasizes the importance of non-vessel water flow in angiosperm trees when the xylem becomes partially blocked.

1 | Introduction

In most terrestrial plants, water flow through the conduits of the vascular system enables leaf gas exchange and productivity. Several processes, like drought (Cochard 2002; Sperry and Tyree 1988), freeze-thawing (Cruiziat et al. 2002; Davis et al. 1999; Ewers et al. 2003; Langan et al. 1997; Pfautsch 2016), fires (Bär et al. 2019), or insect feeding (Carluccio et al. 2023; Sabella et al. 2019), can lead to the blockage of the xylem conduits, impairing water flow and leaf gas exchange. In general, the extent of these impairments increases with the number of blocked conduits and their individual hydraulic conductance. However, there is evidence that the xylem network connectivity and the ability to bypass specific conduits may also play a crucial role (Jacobsen et al. 2024; Loepfe et al. 2007; Mrad et al. 2021; Venturas et al. 2016). This bypassing takes place through lateral pathways (Halis et al. 2012; Tyree et al. 1994), and thereby functions as a central xylem safety mechanism.

The lateral xylem connectivity can vary strongly among species, which has been demonstrated by measures such as (i) the extent of lateral spreading of a dye solution locally injected into the sap flow (Larson et al. 1994; McElrone et al. 2021; Orians et al. 2004; Vite and Rudinsky 1959; Waisel et al. 1972), (ii) the loss of hydraulic conductance after partially blocking axial flow through a stem segment (Ellmore et al. 2006; Zanne et al. 2006), and (iii) the spatial variation in physiological parameters across the canopy in response to non-homogeneous resource distribution in the soil (Orians

et al. 2002; Schenk et al. 2008) or root damaging (Azar et al. 2023; Salguero-Gómez and Casper 2011). Jacobsen et al. (2024) discuss different anatomical traits that determine the lateral xylem connectivity. For vessel-bearing species, these traits include, among others, (i) the arrangement of vessels and (ii) the presence of tracheids. In species with grouped vessels, a few blocked vessels may be bypassed relatively easily through the remaining conductive vessels of that group (Carlquist 1984). In contrast, in species with mostly solitary vessels and few lateral connections among them, blockage of a small number of vessels can lead to the hydraulic isolation of entire sectors. This can be seen in partial root zone drying experiments where the leaf water potential and/or stomatal conductance severely drop in only parts of the canopy, while others remain unaffected (Espino and Schenk 2009). However, when connecting vessels are missing, tracheids, which are present in some but not all vessel-bearing species, may provide alternative water flow pathways (Carlquist 1985). Although narrower and thus less conductive than vessels, tracheids were found to form so-called tracheid-bridges, which enable lateral water transport between vessels (Cai et al. 2014; Pan and Tyree 2019). Interestingly, these two features are expected to be mutually exclusive, since tracheids predominantly exist in species with mostly solitary rather than grouped vessels (Carlquist 2013; Rosell et al. 2007).

Despite those reported differences in xylem anatomical features, it remains unclear to what extent species can differ in their bypassing ability and how relevant those differences are to assess hydraulic limitations after vessel blockage. Here, we investigate the hydraulic bypassing of blocked vessels in two Mediterranean angiosperm tree species, carob (*Ceratonia siliqua*) and oak (*Quercus calliprinos*). The xylem of oaks has been shown to consist mostly of solitary vessels (Ellmore et al. 2006) with additional tracheids present (Percolla et al. 2021). In contrast, carob has a comparably high extent of vessel grouping (Jansen et al. 2011) and thus, presumably, no conducting tracheids. Using oaks and carobs as model species, we aim at answering the following questions:

1. To what extent does the ability to bypass blocked vessels differ between species?
2. What are the hydraulic pathways used for bypassing?

To assess the extent of bypassing, we induced a well-defined portion of blocked vessels by stem notching and measured the resulting effect on gas exchange of leaves attached to the notched side of the stem. Next, we visualized the pathways used for bypassing using microscopy and μCT imaging after dye or tracer injection, respectively. Furthermore, we used macerated stem samples to analyse the cell composition of the xylem of the two species. We hypothesize that the hydraulic impairments caused by a given portion of blocked vessels can significantly differ between different angiosperm tree species, depending on their anatomical features for bypassing.

2 | Materials and Methods

2.1 | Plant Species

The species used in this study were two different Mediterranean angiosperm tree species: common oak (*Quercus calliprinos*) and carob (*Ceratonia siliqua*). Saplings at the age of 1 year were collected from KKL-JNF nursery in Eshtaol, Israel. All plants were 3–7 mm in diameter at 5 cm above root collar, and 20–50 cm in height.

2.2 | Transpiration Measurements of Notched Trees

Saplings of oaks and carobs were grown in pots under controlled temperature and humidity in a climate-controlled walk-in room. Daytime temperature and humidity during the measurement period were on average 27.2°C and 49.3%, respectively. Plants were illuminated for 16 h a day at a PPFD of 800 $\mu mol\, m^{-2}\, s^{-1}$. For each seedling, the side of the stem to be notched was selected and marked. The selection was such that leaf pairs could be found at three different positions of the stem (bottom, mid, top), with each one leaf out of a pair located on the side to be notched, and the other leaf on the opposite, intact side (Figure 1). The overall measurement period covered 13 days. Measurements of stomatal conductance (g_s) were taken on days 0, 5, 6, 7, and 12 at 11.00 am using a leaf porometer (LI-600, LI-COR). On day 6, before 9.00 am, stems were notched. This involved applying multiple notches at 2 cm intervals along the marked side of the stem, including a notch at 3 mm distance below each measured leaf, using a fine hand saw (Figure 1). The depth of the notches was half the stem diameter at each position. In total, we used 12 seedlings per species, out of which eight were notched, and four were kept as controls. At day 13, trees were prepared for imaging of active hydraulic pathways.

2.3 | Microscopy of Stems Immersed in Fuchsine Solution

We used acid fuchsine (Fisher Scientific) solution (1% in degassed mQ water, run through a 20 μm filter) to visualize active water flow pathways in the seedlings used for transpiration measurements. For that, stems were cut at their base while submerged, and then placed in a glass vial containing fuchsine solution. While immersed in the solution, seedlings were allowed to transpire for at least 2 h. We monitored the fuchsine staining at the three marked positions (bottom, mid, top, Figure 1), a few millimeters above the notch and below the selected leaves. The stem was cross-sectioned manually using a fresh razor blade. Cross sections were placed on a microscope slide and photographed under a stereo microscope model SMZ18 (Nikon Instruments). We quantified the stained area of the cross sections of the micrographs using the color threshold tool in ImageJ (Schneider et al. 2012) and normalized it by the total area of the cross-section.

2.4 | μCT Scanning of Stems Immersed in Iohexol Solution

We used μCT scanning with the tracer Iohexol as a complementary technique to visualize water flow pathways (Pratt and Jacobsen 2018) which has been specifically used to examine oak xylem before (Pratt et al. 2019). Compared with microscopy, sample preparation is less invasive, and potential

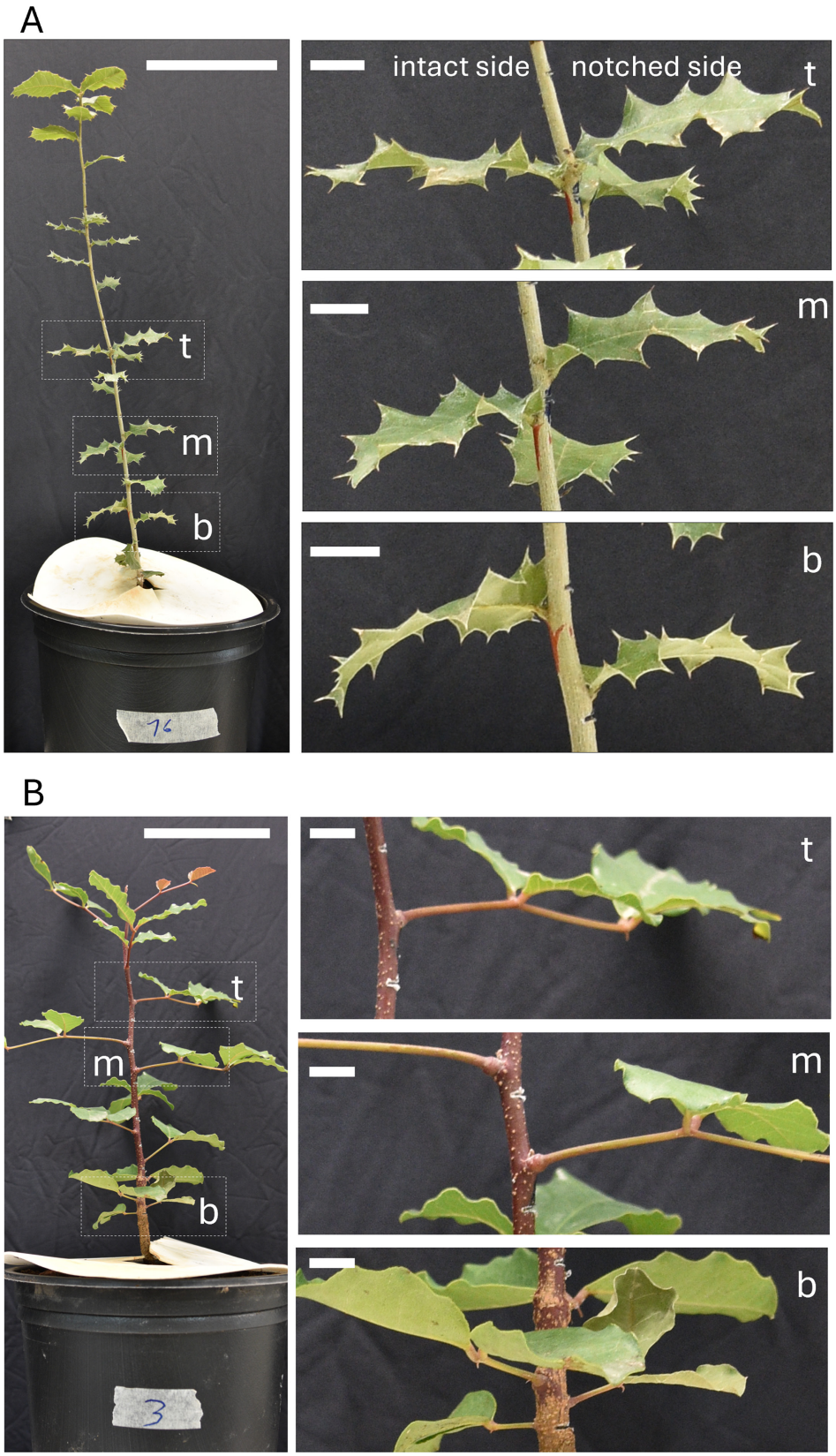

FIGURE 1 | Example of oak (A) and carob (B) seedlings used in the experiment. Per seedling, three leaf pairs were selected; each one from the bottom (b), mid (m), and top (t) parts of the stem. After reference measurements, stems were notched halfway through their cross-section every two centimeters, so that one leaf of the selected pairs was on the notched side, and the other on the intact side of the stem, respectively. Scale bars in the left panels are 10 cm; those in the right panels are 1 cm.

artefacts caused by cross-sectioning are avoided. Additionally, μCT scans allow for a 3D reconstruction of the stem and its conduits. Seedlings selected for this method (five oaks and carobs) were slightly smaller (20–30 cm) than those used for transpiration measurements, due to spatial limitations of the μCT chamber. Growing conditions and the notching procedure were identical. Twenty-four hours after notching, stems were cut under water at their base and put into a glass vial containing Iohexol (Tokyo Chemical Industry Co. Ltd) solution (150 mM in degassed mQ water, run through a 20 μm filter). Seedlings were allowed to transpire for 2 h before scanning. While still immersed in Iohexol solution, seedlings were fixed on a stand, had their canopy covered in tin foil to minimize transpiration, and were placed into the chamber of the μCT device (RX Solutions). Scans were performed under 7 watts with a frame rate of 2 images s^{-1}. The resulting voxel size was 4–7 μm. The field of view selected for imaging ranged from shortly below the notch to above the attached petiole on the notched side of the stem, covering 7 mm in height.

2.5 | Analysing Xylem Cell Composition Using Macerated Stem Samples

To analyze the xylem cell composition, we macerated 1.5 cm long stem segments of oaks ($n = 5$) and carobs ($n = 5$), collected from 5 cm above the stem base. After debarking and pith removal, we put the stem segments for maceration into glass vials containing Jeffreys solution (Schmid 1982). We used a mixture of 1:1 chromic acid (10%) (Fisher Scientific) and nitric acid (10%) (Merck). After incubation for 2–4 days, the solution was removed, and the stem segments were washed 4–5 times with pure water. The disintegrated stem segments were suspended in water, and a drop of the suspension was mounted on a microscope slide and imaged using a light microscope model DM500 (Leica).

2.6 | Imaging of Oak Xylem Using Laser Scanning Confocal Microscopy

We imaged stem cross-sections of two additional oak and carob seedlings using Laser Scanning Confocal Microscopy (LSCM) to visualize the distribution of tracheids at higher resolution. Stems were manually cross-sectioned at 5 cm above the stem base using a fresh razor blade. Cross sections were placed on a microscope slide and imaged with a confocal microscope model A1R HD25 (Nikon Instruments). For imaging, a 20×/0.75 objective was used. We measured the autofluorescence of lignin at an excitation wavelength of 404.1 nm and emission wavelength of 450.0 nm. To account for variation of the optimal focus position in the sample, we collected Z-stacks (25 steps at 0.8 μm intervals). Z-stacks were projected on a 2D image via maximum intensity projection using ImageJ.

2.7 | Imaging of Leaf Traces

We used two additional oak seedlings to image the emergence of leaf traces, bundles of vessels extending from the stem to the leaf. Starting at 2 mm below a leaf node (at around 10 cm above the stem base), stems were consecutively cross-sectioned until reaching the node. Cross sections were placed on a microscope slide and photographed under a stereo microscope model SMZ18 (Nikon Instruments).

2.8 | Statistical Analysis

We used Wilcoxon signed-rank tests to test for significant differences before and after notching in the same group of trees and Mann–Whitney *U* tests to test for significant differences between different groups of trees (i.e., between intact and notched trees or between oaks and carobs). Both types of tests were performed using the SciPy package (Virtanen et al. 2020) in Python.

3 | Results

We measured the effect of consecutively notching stems halfway their cross-section on leaf gas exchange. In both species, notching led to a significant reduction in g_s in leaves on the notched side of the stem at each measured height (Figure 2A–F). However, the extent of the reduction was far stronger in carob, with g_s values decreasing by 68%–100% (Figure 2G,H). At day 6 after notching, most measured leaves had fully stopped transpiring (Figure 2G). In oaks, reductions in g_s were much milder, ranging from 25% to 43%, indicating sustained leaf water supply (Figure 2G,H).

After transpiration measurements, we visualized hydraulic pathways using acid fuchsine as a tracer (Figure 3). Analyzed cross-sections were cut directly above notches, below attached leaves. In intact oak stems, water transport in the stem cross-section was distributed along distinct rays (Figure 3A). Notching the oaks only slightly changed this pattern (Figure 3B). Dye was still present but more diffusely distributed in the notched half of the cross-section than in the intact half. Compared with oak, intact carob seedlings had a more homogeneous dye distribution in the tangential direction, with less distance between rays (Figure 3C). In notched carob seedlings, almost no dye was present in the notched half of the cross-section (Figure 3D), indicating ceased water flow. To quantify the changes in water flow patterns, we calculated the relative area of the cross-section containing dye (Figure 3E–G). In general, dye was more abundant in oak (25%–40%) than in carob stem cross-sections (9%–18%). Notching had no significant effect on dye abundance in oak but tended to increase the portion of stained area. In contrast, in carobs, notching caused a significant decrease in dye abundance at the bottom and mid of the stem from 17% to 12%, and from 14% to 10%, respectively.

Micrographs taken at greater magnification revealed additional differences in water flow patterns between oak and carob (Figure 4). Vessels in oak were mostly solitary, whereas in carob most vessels occurred in clustered groups. In oak, not only vessels but also the surrounding cells contained dye, leading to a continuous staining along rays (Figure 4A–D). This indicates that the surrounding cells were involved in water transport. These can form lateral hydraulic connections between rays containing vessels (Figure 4D). In carob, however, dye appears only in close proximity to vessels and not in the surrounding cells. This indicates that water flows exclusively through vessels. Hence, there is no visible lateral hydraulic connection between distinct groups of vessels.

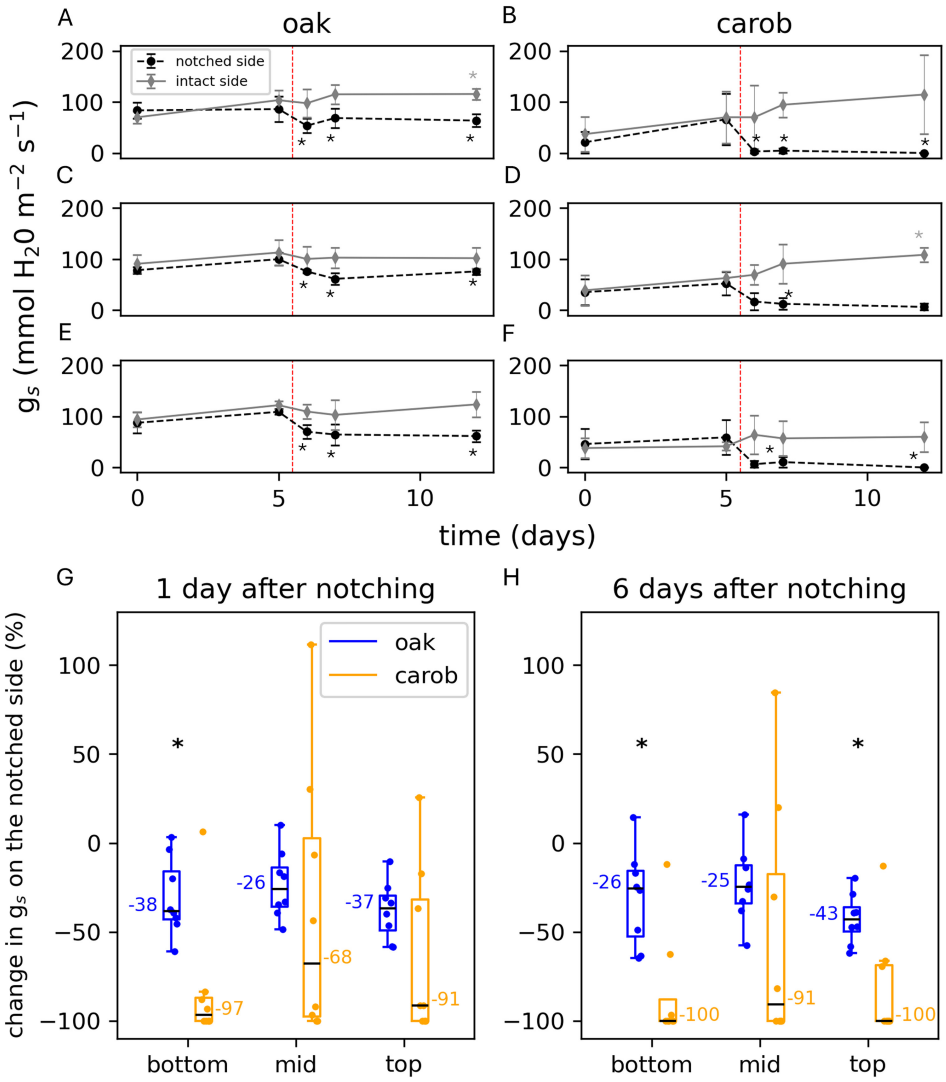

FIGURE 2 | The effect of stem notching on stomatal conductance compared between oak and carob saplings ($n = 8$). Per plant, three leaf pairs were selected at different heights of the stem (bottom, mid, top), with one leaf on the side to notch, and the other one on the opposite side. (A–F) show the dynamics of gs over time, including two time points before (0 and 5 days) and three time points after (6, 7, and 12 days) notching. Leaf pairs from three different positions at the stem were measured: Bottom (A, B), mid (C, D), and top (E, F). Points are median values, error bars are median absolute deviations. The red vertical line indicates the time point of notching. Asterisks indicate significant differences in gs of leaves on the notched (grey asterisks) and intact side (black asterisks) at each measured day after notching compared with d5, tested by a Wilcoxon signed-rank test ($p < 0.05$). (G, H) show changes in gs of leaves from the notched side in % (6 and 12 days compared to 5 days). Horizontal lines are medians, boxes reach from the first to the third quartile. Whiskers mark the minimal and maximal data points within 1.5 times the interquartile range from the first and third quartile, respectively. Asterisks indicate significant differences between oak and carob at each height, tested by a Mann–Whitney *U* test ($p < 0.05$).

We used μCT imaging after introducing Iohexol solution into the transpiration stream as an additional method to visualize water flow pathways (Figure 5). Areas in the cross-section that contain Iohexol appear brighter and indicate active water flow pathways. Embolized (hollow) vessels appear as dark spots. Figure 5 shows cross sections from 1 mm below the notch (Figure 5A–D), 1 mm above the notch (Figure 5E–H), and 6 mm above the notch (Figure 5I–L) of two example oaks (left columns) and carobs (right columns). In oaks, Iohexol in the intact half of the cross-section was distributed along rays. Spots with a greater intensity indicate vessels within these rays (e.g., white arrow in Figure 5E). Iohexol was also present in cells outside vessels within rays, but much less in the spaces in between rays. In the notched side of the cross-section, most vessels were embolized (e.g., black arrow in Figure 5E). However, Iohexol was still present around vessels, indicating active water flow pathways. Additionally, Iohexol was detected in the spaces in between rays, indicating tangentially oriented hydraulic pathways (e.g., orange arrows in Figure 5E). Compared with the intact half, Iohexol outside vessels in the notched half at 1 mm above the notch (Figure 5E,F) showed a greater intensity. In carobs, Iohexol in the intact half was only present in vessels (e.g., white arrow in Figure 5G) but not in the surrounding cells. In the notched half, most vessels were embolized (e.g., black arrow in Figure 5G). Iohexol was only scarcely present in the notched half and appeared in patches outside vessels (e.g., orange arrow in Figure 5G). However, in contrast to oaks, large parts of the notched half in carobs did not contain Iohexol, indicating ceased water flow.

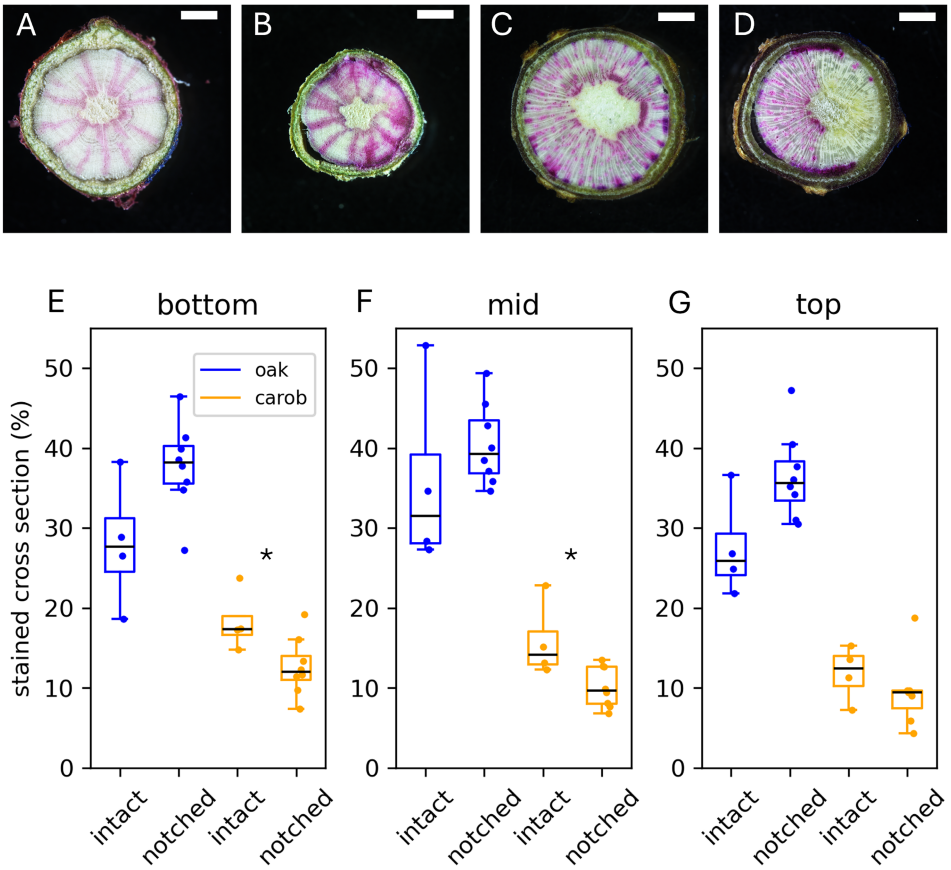

FIGURE 3 | Fuchsine distribution in the stem cross-section indicating active water flow pathways. Example microscopy images of stem cross sections of an intact oak (A, $n = 4$), notched oak (B, $n = 8$), intact carob (C, $n = 4$), and notched carob (D, $n = 8$). Shown cross sections are from the 'bottom' position. Cross sections from notched trees are oriented with the notched side on the right. Scale bars are 1 mm. The relative area of the cross-section containing fuchsine was quantified using ImageJ software. Results are shown in (E–G). Horizontal lines are medians, boxes reach from the first to the third quartile. Whiskers mark the minimal and maximal data points within 1.5 times the interquartile range from the first and third quartiles, respectively. Asterisks indicate significant differences between intact and notched trees of the same species, tested by a Mann–Whitney *U* test ($p < 0.05$).

We determined the cell composition of the xylem using microscopy of macerated stem segments (Figure 6). For both oaks and carobs, we identified vessel elements (Figure 6B,F) and fibers (Figure 6C,G). Tracheids with bordered pits were abundant only in oaks (Figure 6D) but not in carobs. Besides vessel elements and fibers, we observed a third type of elongated cells in carobs (Figure 6H), which likely are parenchyma-like fibers (Kumar and Gupta 2023).

After identification of the different xylem cell types, we mapped their distribution in the stem cross-section using LSCM for better optical resolution (Figure 7). In oaks, vessels were solitary and surrounded by cells that likely are tracheids and fibers (Figure 7A). Although a clear distinction between the two is difficult due to their similar diameter (compare Figure 6A), we classified those with bigger lumen as tracheids and those with thinner lumen and thicker walls as fibers. Following this classification, we found tracheids to form tangentially oriented arrays connected to vessels (Figure 7C). In the radial direction, there were alternating arrays of tracheids and axial parenchyma. In carobs, vessels were arranged as grouped vessels surrounded by fibers and parenchyma cells (Figure 7B,D). Compared with the tracheids in oaks, fibers in carob had a smaller lumen and thicker cell walls.

We imaged the emergence of leaf traces in oak using microscopy on stem cross sections directly below the leaf node (Figure S1). Additionally, we used cross sections of the μCT scans with Iohexol on notched oak stems with the leaf node directly above the notch (Figure S2). Both methods show that there was a single leaf trace per node emerging from the same side of the stem cross-section as the node. Furthermore, the μCT scans show that the leaf trace contained Iohexol, indicating active water flow while at least parts of the vessels in the leaf trace were embolized (Figure S2).

4 | Discussion

We measured the effect of stem notching on leaf gas exchange in seedlings of two different angiosperm tree species (oak and carob) to assess their ability to bypass blocked vessels. In oaks, leaves on the notched side of the stem kept their stomatal conductance at more than 50% as compared to before notching (Figure 2). Water flow pathways in the notched half of the stem were active (Figures 3 and 5). In contrast, in carobs, stomatal conductance in leaves on the notched side of the stem dropped to close to zero (Figure 2). In addition, water flow in the notched

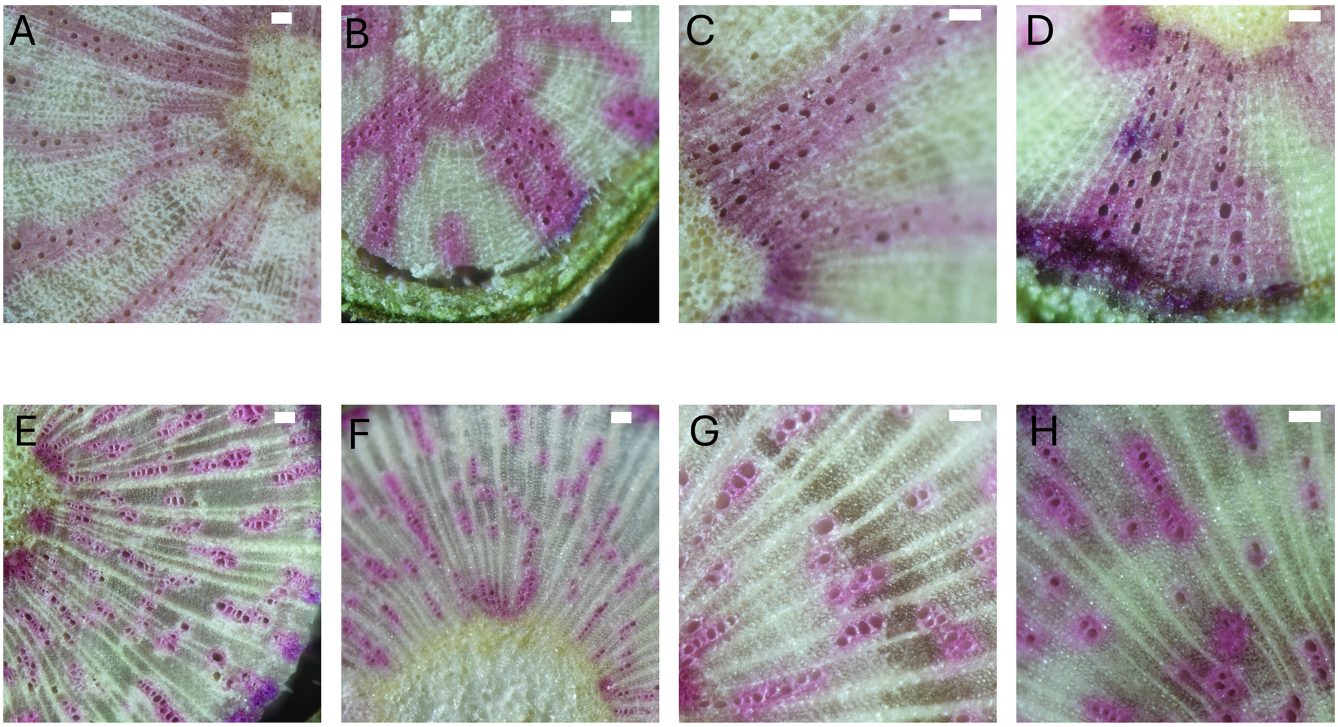

FIGURE 4 | Fuchsine distribution in the stem cross-section indicating active water flow pathways in intact example oaks (A–D) and carobs (E–H). Vessels appear as black circles. Scale bars are 100 μm.

half had ceased (Figures 3 and 5). These results demonstrate that the hydraulic impairments caused by a given loss of conductive vessels can be highly species-specific, depending on their capability for bypassing.

In vessel-bearing species, high lateral xylem connectivity, and thus high potential for bypassing is associated with both vessel grouping and the presence of vasicentric tracheids (Carlquist 1984, 1985; Jacobsen et al. 2024). Compared to other species, oaks were shown to have a low extent of vessel grouping with few connecting vessels in lateral direction (Ellmore et al. 2006). In agreement with that, we found vessels in oaks to be arranged almost exclusively as solitary vessels without adjacent neighbours in the stem cross-section (Figures 4, 5, and 7). In carobs, however, most vessels were grouped, and solitary vessels were rarely present (Figures 4, 5, and 7). Thus, based on the arrangement of vessels alone, we would expect more effective bypassing in carobs than in oaks. Since this is opposite to our findings, we conclude that vessel arrangement alone was not the decisive factor for bypassing in our study, confirming previously reported results (Mrad et al. 2021).

As indicated by imaging active hydraulic pathways, water transport in carobs was almost exclusively via vessels (Figures 4 and 5). In oaks, however, cells surrounding vessels were also involved in water transport and formed lateral connections between adjacent rays of vessels (Figures 4 and 5). These differences in water flow patterns can be explained by the abundance of tracheids with bordered pits, which were present in oaks but not in carobs (Figure 6). This fits the observation from Carlquist (2013) that species with solitary vessels, rather than species with grouped vessels, tend to have additional tracheids. Specifically for oaks, the presence of tracheids and their contribution to water flow have been pointed out before (Percolla et al. 2021). Our data indicate that bypassing blocked vessels to ensure leaf water supply in oaks was indeed dependent on tracheid flow: μCT scans of notched oak stems show tangentially oriented active hydraulic pathways between adjacent rays in the notched half of the stem (Figure 5E). This corresponds with the tangentially oriented distribution of arrays of tracheids in the cross-section of oak stems (Figure 7). In radial direction, conductive tracheids alternate with arrays of axial parenchyma (Figure 7), which explains the pattern of the Iohexol signal in the μCT scans (Figure 5E). Furthermore, we found that oaks had only one leaf trace per node emerging from the same side of the stem as the node (Figure S2). Thus, water supply could not be realized through vessels directly leading from the intact side of the stem to the leaf on the notched half. We therefore conclude that bypassing embolized vessels in oaks was enabled by the presence of tracheids forming lateral hydraulic pathways. This bypassing was sufficient to keep stomatal conductance of leaves on the notched side at more than 50% under conditions of well-watered soil and moderate vapour pressure deficit (2 kPa).

In our study, the presence of tracheids had a greater impact on the ability to bypass than the extent of vessel grouping. This might partly be due to the highly inhomogeneous pattern of vessel blockage that we induced by notching half of the stem cross-section. One half of all groups of vessels in carobs was fully embolized and the other half was fully conductive (Figures 3 and 5). This left almost no possibilities to bypass a blockage within a group through parallel, redundant vessels. If we had instead induced embolism in 50% of vessels in each group, bypassing in carobs may have been more efficient. However, vessel blockage under natural conditions can occur in patches too. This is because embolism can spread from one

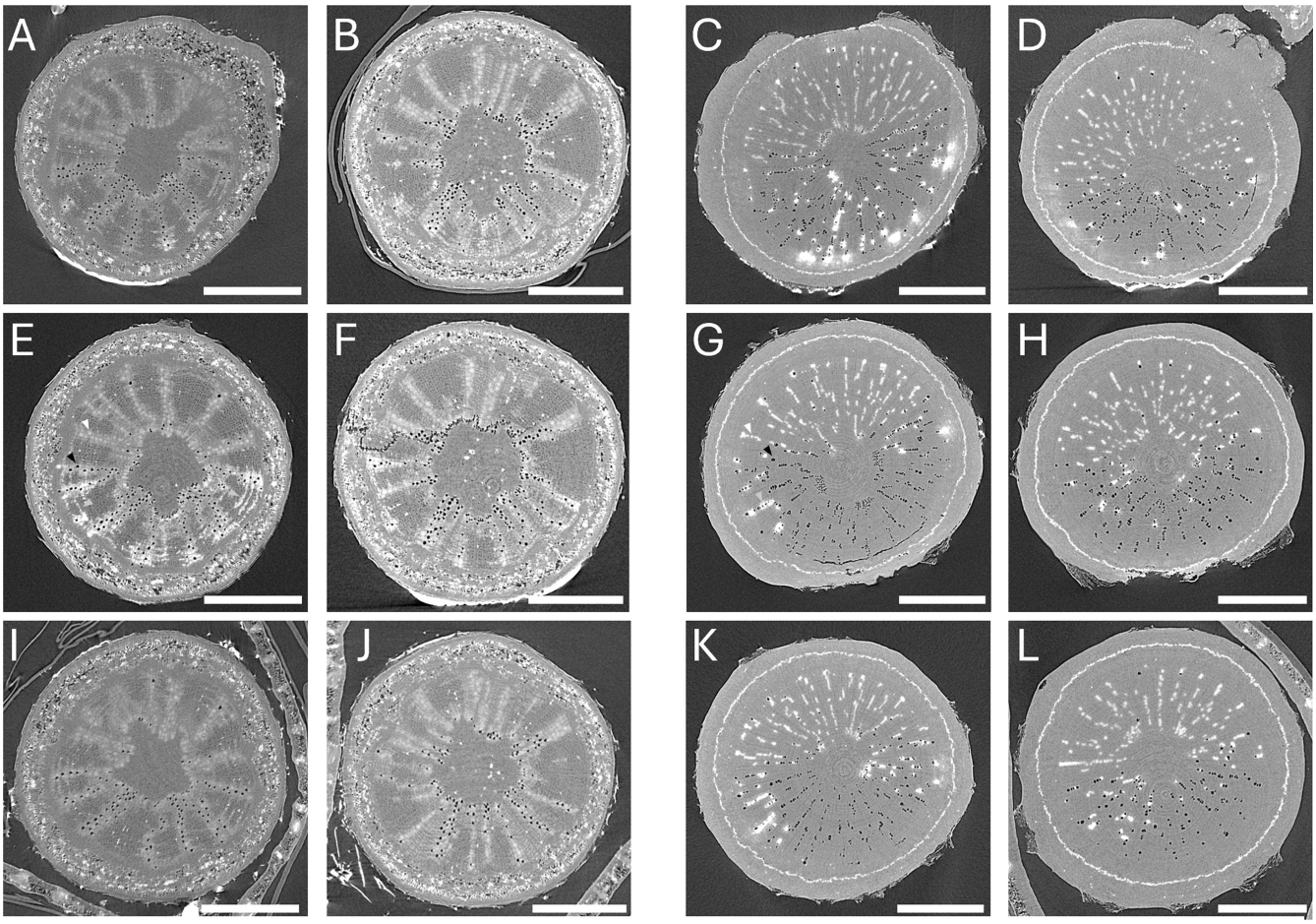

FIGURE 5 | Cross sections of uCT scans of two oak (A, B, E, F, I, G) and two carob (C, D, H, G, K, L) stems after notching. Iohexol solution was fed to the stem as a contrast agent. Areas containing Iohexol appear brighter. White arrows in (E, G) indicate Iohexol-filled vessels, black arrows indicate gas-filled vessels. Orange arrows in (E, G) indicate Iohexol outside vessels. Cross sections are from 1 mm below the notch (A–D), 1 mm above the notch (E–H) and 6 mm above the notch (I–L). Stems are oriented with the notched half towards the bottom. Scale bars are 1 mm.

vessel to its neighbours (Guan et al. 2021; Knipfer et al. 2015; Sperry and Tyree 1988), which is especially prominent in species with grouped vessels (Loepfe et al. 2007). Moreover, tracheids, compared with vessels, are more resistant to embolism due to their fewer pits (Pratt et al. 2023 and references within). Therefore, both the embolism patterns we artificially induced here, patches of embolized vessel groups in carobs and embolized solitary vessels surrounded by conducting tracheids in oaks, likely occur under natural conditions too, albeit to a lesser extent than in our study.

Hence, our findings may have implications for the assessment of drought-induced embolism, probably the most-widely studied process leading to vessel blockage. A common method to assess a tree's drought resilience is based on its vulnerability curve, that is, the relation between the percentage loss of conductance (PLC) caused by embolism and the water deficit measured as plant water potential (Awad et al. 2010; Choat et al. 2012; Cochard et al. 2008; Larter et al. 2024; Pockman and Sperry 2000; Wagner et al. 2022, 2023). The lower the PLC at a given water potential, the more drought resilient a species is considered. Furthermore, it has been reported that the extent of embolism is the main determinant of a plant's ability to recover from drought and the time required for it, with fixed thresholds among a large range of species from the same clade (Brodribb and Cochard 2009; Urli et al. 2013). Our study indicates that two different species from the same clade can differ significantly in the hydraulic impairment caused by a given extent of embolism. Due to bypassing through tracheids, the same portion of blocked vessels led to much milder limitations in leaf water supply in oaks than in carobs. The question arises if these differences would be captured in vulnerability curves. Compared to water flow through vessels, the contribution of tracheid flow to the total axial conductance of a stem segment is generally low, ranging only up to 2.2% (Pan and Tyree 2019), although greater values (5.7%–15.5%) were reported specifically for oaks (Percolla et al. 2021). Thus, only considering axial tracheid transport, the PLC for a given portion of embolized vessels is expected to be slightly lower for species with additional tracheids. A more striking effect may result from so-called tracheid bridges which were shown to effectively connect vessels in lateral direction without inducing much additional resistance (Cai et al. 2014; Pan and Tyree 2019), probably due to the comparably short lateral path length. Hence, if a stem segment contains conductive vessels connected to embolized ones, the hydraulically measured PLC is expected to be considerably lower when lateral tracheid bridges are present. Similarly, Jacobsen et al. (2024) argue that

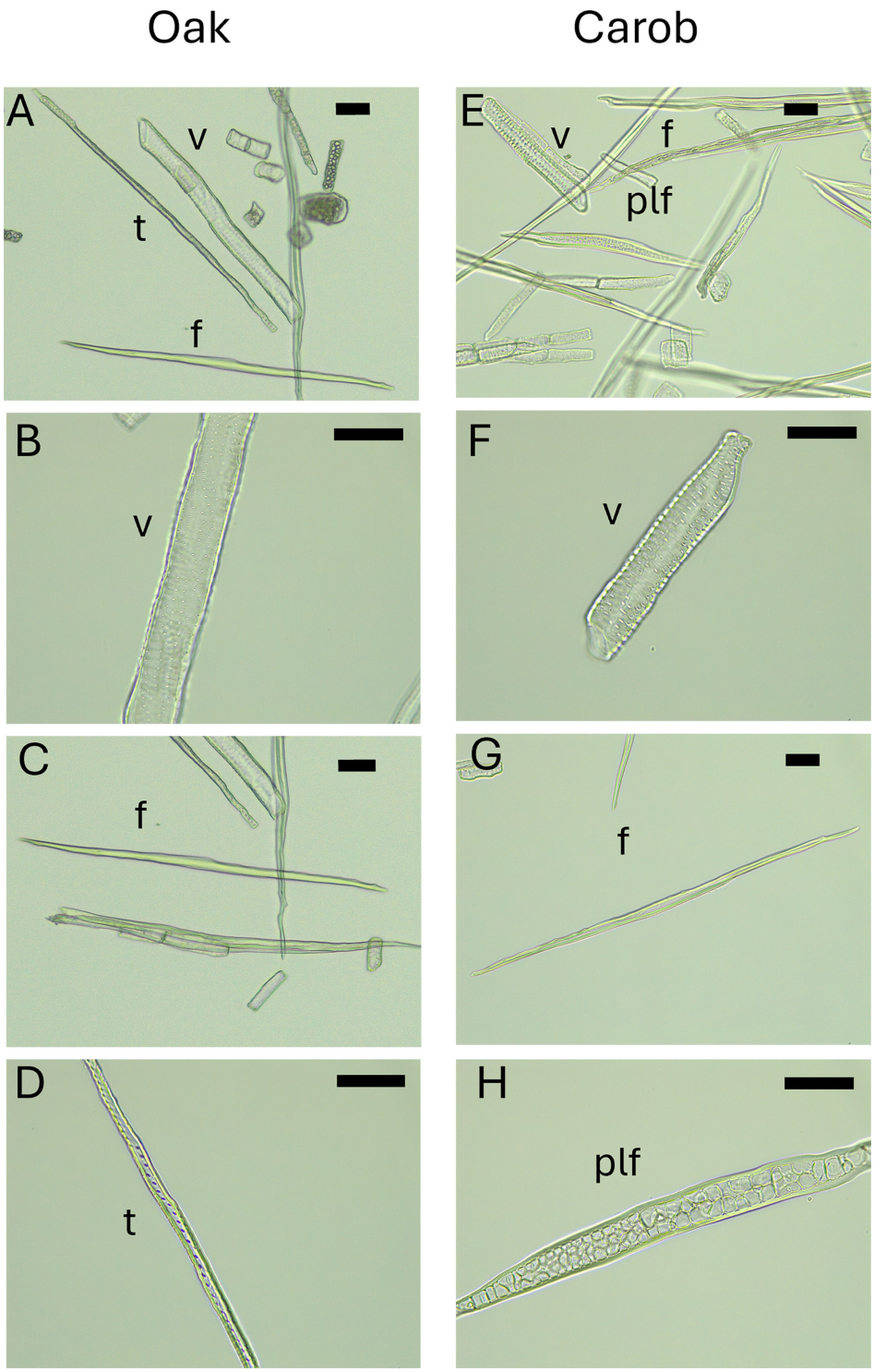

FIGURE 6 | Example micrographs of cell suspensions obtained from macerated xylem samples of oaks (A–D) and carobs (E–H). Identified cell types were vessel elements (v), fibers (f), tracheids with bordered pits (t), and parenchyma-like fibers (plf). Scale bar is 50 μm.

low xylem connectivity, for example, for trees without vasicentric tracheids, can lead to an underestimation of the PLC when assessed visually using Hagen Poiseuille estimates based on, for example, μCT images. This is because not only the embolized vessels themselves but also those connected to them could be cut off from water transport. We therefore think that the effect of bypassing blocked vessels is reflected in vulnerability curves depending on the distribution of embolism and the method used to assess PLC. For our setup, it is likely that oaks and carobs would have a similar PLC since in both species all vessels in one half of the stem were embolized along their full height. The bypassing we found in oaks was from the intact half of the stem into the petiole of leaves on the notched half, a pathway usually not captured in standard PLC measurements.

Although the pattern of vessel blockage we induced here is artificial and most likely differs from that caused by naturally induced embolism during drought, our findings suggest that

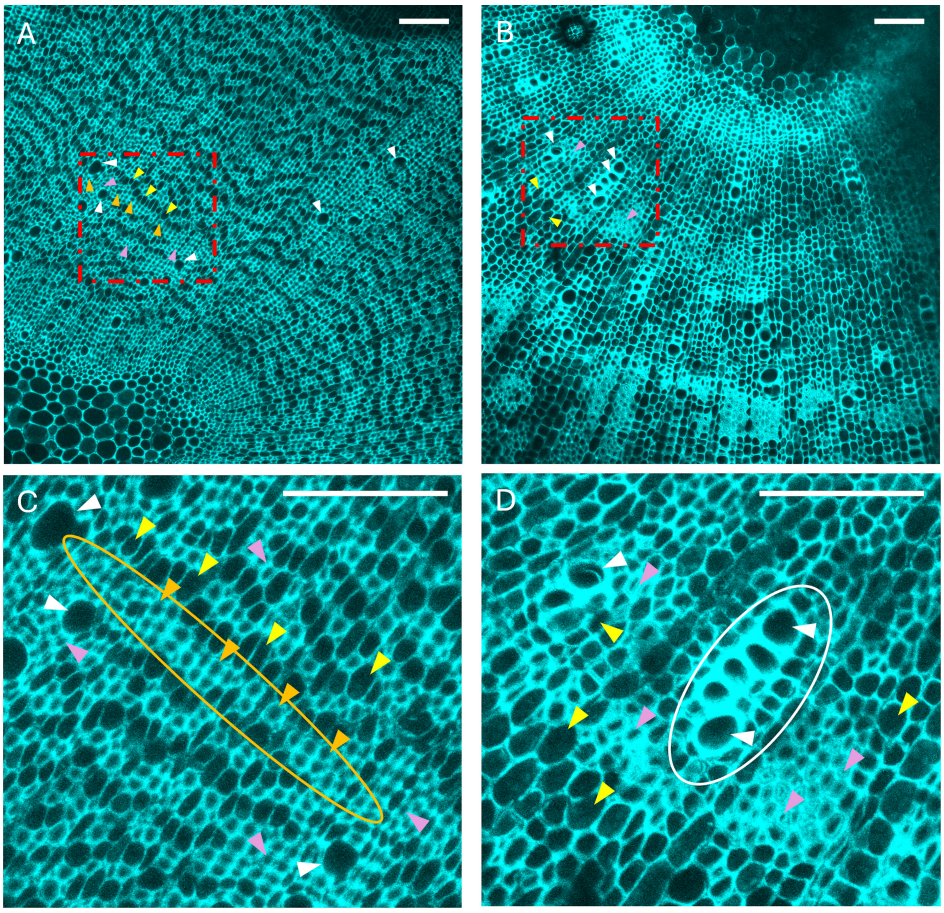

FIGURE 7 | Cross sections of oak (A, C) and carob (B, D) stems showing the distribution of vessels (white arrows), tracheids (orange arrows), parenchyma cells (yellow arrows) and fibers (pink arrows). (C, D) are magnifications of the sections marked by the red rectangles in (A, B), respectively. The orange ellipse in (C) indicates a tangentially oriented array of tracheids and fibers. The white ellipse in (D) indicates a group of vessels. Images are maximum projections of z-stacks measured with Laser Scanning Confocal Microscopy. The signal shown is the autofluorescence of lignin in the cell walls (excitation wavelength: 404.1 nm, emission wavelength: 450.0 nm). Scale bars are 100 μm.

considering a species' ability for bypassing blocked vessels to ensure leaf water supply can complement drought resilience assessments based on PLC measurements. Supporting this, we found that carobs die from drought with less than 40% embolism (Wagner et al., under review) while oaks were reported to survive much higher degrees of embolism (Carevic et al. 2014; Peguero-Pina et al. 2018). Hence, we argue in line with Carlquist (1985) that the presence of tracheids considerably contributes to the drought resilience of vessel-bearing species. The potential ecological relevance of this feature is indicated by two studies reporting that 70%–76% of different subsets of vessel-bearing species have tracheids (Rosell et al. 2007; Ziemińska 2023). Therefore, we recommend integrating knowledge from wood anatomy and physiology when assessing the resilience of forests to disturbances like drought, freezing, fires, or mechanical damage. In turn, effects like blockage bypassing should be parameterized into forest process models.

Author Contributions

Y.M. planned the research and performed the experiment, analysis, and manuscript writing under the guidance of T.K. G.P. performed the xylem maceration and imaging. U.H. consulted during all steps.

Acknowledgements

We thank Yael Wagner for her critical comments which helped to improve the manuscript and Gil Feiguelman for his help with the confocal microscopy.

Funding

The study was facilitated by the European Research Council grant RESILFOREST. YM is supported by the Institute for Environmental Sustainability (IES) at the Weizmann Institute of Science. HORIZON EUROPE European Research Council.

Disclosure

No AI has been used in any form for preparing this manuscript.

Data Availability Statement

The data that support the findings of this study are available from the corresponding author upon reasonable request.

References

Awad, H., T. Barigah, E. Badel, H. Cochard, and S. Herbette. 2010. "Poplar Vulnerability to Xylem Cavitation Acclimates to Drier Soil Conditions." *Physiologia Plantarum* 139, no. 3: 280–288. https://doi.org/10.1111/j.1399-3054.2010.01367.x.

Azar, M., G. Mulero, Y. Oppenheimer-Shaanan, D. Helman, and T. Klein. 2023. "Aboveground Responses to Belowground Root Damage Detected by Non-Destructive Sensing Metrics in Three Tree Species." *Forestry* 96, no. 5: 672–689. https://doi.org/10.1093/forestry/cpad002.

Bär, A., S. T. Michaletz, and S. Mayr. 2019. "Fire Effects on Tree Physiology." *New Phytologist* 223, no. 4: 1728–1741. https://doi.org/10.1111/nph.15871.

Brodribb, T. J., and H. Cochard. 2009. "Hydraulic Failure Defines the Recovery and Point of Death in Water-Stressed Conifers." *Plant Physiology* 149, no. 1: 575–584. https://doi.org/10.1104/pp.108.129783.

Cai, J., S. Li, H. Zhang, S. Zhang, and M. T. Tyree. 2014. "Recalcitrant Vulnerability Curves: Methods of Analysis and the Concept of Fibre Bridges for Enhanced Cavitation Resistance." *Plant, Cell & Environment* 37, no. 1: 35–44. https://doi.org/10.1111/pce.12120.

Carevic, F., M. Fernández, R. Alejano, and J. Vázquez-Piqué. 2014. "Xylem Cavitation Affects the Recovery of Plant Water Status and Consequently Acorn Production in a Holm Oak Open Woodland." *Acta Physiologiae Plantarum* 36, no. 12: 3283–3290. https://doi.org/10.1007/s11738-014-1694-6.

Carlquist, S. 1984. "Vessel Grouping in Dicotyledon Wood." *Aliso: A Journal of Systematic and Floristic Botany* 10, no. 4: 505–525.

Carlquist, S. 1985. "Vasicentric Tracheids as a Drought Survival Mechanism in the Woody Flora of Southern California and Similar Regions; Review of Vasicentric Tracheids." *Botany Commons Recommended Citation Recommended Citation Carlquist* 11, no. 1: 37–68.

Carlquist, S. 2013. *Comparative Wood Anatomy: Systematic, Ecological, and Evolutionary Aspects of Dicotyledon Wood*. Springer Science & Business Media.

Carluccio, G., D. Greco, E. Sabella, M. Vergine, L. De Bellis, and A. Luvisi. 2023. "Xylem Embolism and Pathogens: Can the Vessel Anatomy of Woody Plants Contribute to *X. fastidiosa* Resistance?" *Pathogens* 12, no. 6: 825. https://doi.org/10.3390/pathogens12060825.

Choat, B., S. Jansen, T. J. Brodribb, et al. 2012. "Global Convergence in the Vulnerability of Forests to Drought." *Nature* 491, no. 7426: 752–755. https://doi.org/10.1038/nature11688.

Cochard, H. 2002. "Xylem Embolism and Drought-Induced Stomatal Closure in Maize." *Planta* 215, no. 3: 466–471. https://doi.org/10.1007/s00425-002-0766-9.

Cochard, H., S. T. Barigah, M. Kleinhentz, and A. Eshel. 2008. "Is Xylem Cavitation Resistance a Relevant Criterion for Screening Drought Resistance Among Prunus Species?" *Journal of Plant Physiology* 165, no. 9: 976–982. https://doi.org/10.1016/j.jplph.2007.07.020.

Cruiziat, P., H. Cochard, and T. Améglio. 2002. "Hydraulic Architecture of Trees: Main Concepts and Results." *Annals of Forest Science* 59, no. 7: 723–752. https://doi.org/10.1051/forest:2002060.

Davis, S. D., J. S. Sperry, and U. G. Hacke. 1999. "The Relationship Between Xylem Conduit Diameter and Cavitation Caused by Freezing." *American Journal of Botany* 86, no. 10: 1367–1372. https://doi.org/10.2307/2656919.

Ellmore, G. S., A. E. Zanne, and C. M. Orians. 2006. "Comparative Sectoriality in Temperate Hardwoods: Hydraulics and Xylem Anatomy." *Botanical Journal of the Linnean Society* 150, no. 1: 61–71.

Espino, S., and H. J. Schenk. 2009. "Hydraulically Integrated or Modular? Comparing Whole-Plant-Level Hydraulic Systems Between Two Desert Shrub Species With Different Growth Forms." *New Phytologist* 183, no. 1: 142–152. https://doi.org/10.1111/j.1469-8137.2009.02828.x.

Ewers, F. W., M. C. Lawson, T. J. Bowen, and S. D. Davis. 2003. "Freeze/Thaw Stress in Ceanothus of Southern California Chaparral." *Oecologia* 136, no. 2: 213–219. https://doi.org/10.1007/s00442-003-1273-9.

Guan, X., L. Pereira, S. A. M. McAdam, K. F. Cao, and S. Jansen. 2021. "No Gas Source, no Problem: Proximity to Pre-Existing Embolism and Segmentation Affect Embolism Spreading in Angiosperm Xylem by Gas Diffusion." *Plant, Cell & Environment* 44, no. 5: 1329–1345. https://doi.org/10.1111/pce.14016.

Halis, Y., S. Djehichi, and M. M. Senoussi. 2012. "Vessel Development and the Importance of Lateral Flow in Water Transport Within Developing Bundles of Current-Year Shoots of Grapevine (*Vitis Vinifera* L.)." *Trees* 26, no. 3: 705–714. https://doi.org/10.1007/s00468-011-0637-8.

Jacobsen, A. L., M. D. Venturas, U. G. Hacke, and R. B. Pratt. 2024. "Sap Flow Through Partially Embolized Xylem Vessel Networks." *Plant, Cell & Environment* 47, no. 9: 3375–3392. https://doi.org/10.1111/pce.14990.

Jansen, S., E. Gortan, F. Lens, et al. 2011. "Do Quantitative Vessel and Pit Characters Account for Ion-Mediated Changes in the Hydraulic Conductance of Angiosperm Xylem?" *New Phytologist* 189, no. 1: 218–228. https://doi.org/10.1111/j.1469-8137.2010.03448.x.

Knipfer, T., C. R. Brodersen, A. Zedan, D. A. Kluepfel, and A. J. McElrone. 2015. "Patterns of Drought-Induced Embolism Formation and Spread in Living Walnut Saplings Visualized Using X-Ray Microtomography." *Tree Physiology* 35, no. 7: 744–755. https://doi.org/10.1093/treephys/tpv040.

Kumar, D., and S. Gupta. 2023. "Occurrence of Parenchyma-Like Fibres (PLFs) in Secondary Xylem of Selected Indian Hardwoods." *Journal of the Indian Academy of Wood Science* 20, no. 1: 89–106. https://doi.org/10.1007/s13196-022-00305-8.

Langan, S. J., F. W. Ewers, and S. D. Davis. 1997. "Xylem Dysfunction Caused by Water Stress and Freezing in Two Species of Co-Occurring Chaparral Shrubs." *Plant, Cell & Environment* 20, no. 4: 425–437. https://doi.org/10.1046/j.1365-3040.1997.d01-94.x.

Larson, D. W., J. Doubt, and U. Matthes Sears. 1994. "Radially Sectored Hydraulic Pathways in the Xylem of *Thuja occidentalis* as Revealed by the Use of Dyes." *International Journal of Plant Sciences* 155, no. 5: 569–582.

Larter, M., A. Akhmedov, C. Payne, S. Delzon, and T. Klein. 2024. "High and Variable Hydraulic Resistance to Embolism Among Three Asian Juniper Species." *Journal of Plant Hydraulics* 10, no. 1: 2. https://doi.org/10.20870/jph.2024.2.

Loepfe, L., J. Martinez-Vilalta, J. Piñol, and M. Mencuccini. 2007. "The Relevance of Xylem Network Structure for Plant Hydraulic Efficiency and Safety." *Journal of Theoretical Biology* 247, no. 4: 788–803. https://doi.org/10.1016/j.jtbi.2007.03.036.

McElrone, A. J., C. M. Manuck, C. R. Brodersen, A. Patakas, K. R. Pearsall, and L. E. Williams. 2021. "Functional Hydraulic Sectoring in Grapevines as Evidenced by Sap Flow, Dye Infusion, Leaf Removal and Micro-Computed Tomography." *AoB Plants* 13, no. 2: plab003. https://doi.org/10.1093/aobpla/plab003.

Mrad, A., D. M. Johnson, D. M. Love, and J. C. Domec. 2021. "The Roles of Conduit Redundancy and Connectivity in Xylem Hydraulic Functions." *New Phytologist* 231, no. 3: 996–1007. https://doi.org/10.1111/nph.17429.

Orians, C. M., M. Ardón, and B. A. Mohammad. 2002. "Vascular Architecture and Patchy Nutrient Availability Generate Within-Plant Heterogeneity in Plant Traits Important to Herbivores." *American Journal of Botany* 89, no. 2: 270–278. https://doi.org/10.3732/ajb.89.2.270.

Orians, C. M., M. M. I. Van Vuuren, N. L. Harris, B. A. Babst, and G. S. Ellmore. 2004. "Differential Sectoriality in Long-Distance Transport in Temperate Tree Species: Evidence From Dye Flow, 15N Transport, and Vessel Element Pitting." *Trees* 18, no. 5: 501–509. https://doi.org/10.1007/s00468-004-0326-y.

Pan, R., and M. T. Tyree. 2019. "How Does Water Flow From Vessel to Vessel? Further Investigation of the Tracheid Bridge Concept." *Tree Physiology* 39, no. 6: 1019–1031. https://doi.org/10.1093/treephys/tpz015.

Peguero-Pina, J. J., Ó. Mendoza-Herrer, E. Gil-Pelegrín, and D. Sancho-Knapik. 2018. "Cavitation Limits the Recovery of Gas Exchange After

Severe Drought Stress in Holm Oak (*Quercus ilex* L.)." *Forests* 9, no. 8: 443. https://doi.org/10.3390/f9080443.

Percolla, M. I., J. C. Fickle, F. D. Rodríguez-Zaccaro, R. B. Pratt, and A. L. Jacobsen. 2021. "Hydraulic Function and Conduit Structure in the Xylem of Five Oak Species." *IAWA Journal* 42, no. 3: 279–298. https://doi.org/10.1163/22941932-bja10059.

Pfautsch, S. 2016. "Hydraulic Anatomy and Function of Trees—Basics and Critical Developments." *Current Forestry Reports* 2, no. 4: 236–248. https://doi.org/10.1007/s40725-016-0046-8.

Pockman, W. T., and J. S. Sperry. 2000. "Vulnerability to Xylem Cavitation and the Distribution of Sonoran Desert Vegetation." *American Journal of Botany* 87, no. 9: 1287–1299. https://doi.org/10.2307/2656722.

Pratt, R. B., V. Castro, J. C. Fickle, and A. L. Jacobsen. 2019. "Embolism Resistance of Different Aged Stems of a California Oak Species (*Quercus douglasii*): Optical and microCT Methods Differ From the Benchtop-Dehydration Standard." *Tree Physiology* 40, no. 1: 5–18. https://doi.org/10.1093/treephys/tpz092.

Pratt, R. B., V. Castro, and A. L. Jacobsen. 2023. "The Functional Significance of Tracheids Co-Occurring With Vessels in Xylem of Eudicots Suggests a Role in Embolism Tolerance." *IAWA Journal* 6, no. 4: 1–18. https://doi.org/10.1163/22941932-bja10111.

Pratt, R. B., and A. L. Jacobsen. 2018. "Identifying Which Conduits Are Moving Water in Woody Plants: A New HRCT-Based Method." *Tree Physiology* 38, no. 8: 1200–1212. https://doi.org/10.1093/treephys/tpy034.

Rosell, J. A., M. E. Olson, R. Aguirre-Hernández, and S. C. Fls. 2007. "Logistic Regression in Comparative Wood Anatomy: Tracheid Types, Wood Anatomical Terminology, and New Inferences From the Carlquist and Hoekman Southern Californian Data Set." *Botanical Journal of the Linnean Society* 154: 331–351. https://academic.oup.com/botlinnean/article/154/3/331/2420315.

Sabella, E., A. Aprile, A. Genga, et al. 2019. "Xylem Cavitation Susceptibility and Refilling Mechanisms in Olive Trees Infected by *Xylella fastidiosa*." *Scientific Reports* 9: 9602. https://doi.org/10.1038/s41598-019-46092-0.

Salguero-Gómez, R., and B. B. Casper. 2011. "A Hydraulic Explanation for Size-Specific Plant Shrinkage: Developmental Hydraulic Sectoriality." *New Phytologist* 189, no. 1: 229–240. https://doi.org/10.1111/j.1469-8137.2010.03447.x.

Schenk, H. J., S. Espino, C. M. Goedhart, M. Nordenstahl, H. I. Martinez Cabrera, and C. S. Jones. 2008. "Hydraulic Integration and Shrub Growth Form Linked Across Continental Aridity Gradients." *Proceedings of the National Academy of Sciences of the United States of America* 105, no. 32: 11248–11253. https://doi.org/10.1073/pnas.0804294105.

Schmid, R. 1982. "Sonication and Other Improvements on Jeffrey's Technique for Macerating Wood." *Biotechnic and Histochemistry* 57, no. 5: 293–299. https://doi.org/10.3109/10520298209066726.

Schneider, C. A., W. S. Rasband, and K. W. Eliceiri. 2012. "NIH Image to ImageJ: 25 Years of Image Analysis." *Nature Methods* 9, no. 7: 671–675. https://doi.org/10.1038/nmeth.2089.

Sperry, J. S., and M. T. Tyree. 1988. "Mechanism of Water Stress-Induced Xylem Embolism1." *Plant Physiology* 88, no. 3: 581–587.

Tyree, M. T., S. D. Davis, and H. Cochard. 1994. "Biophysical Perspectives of Xylem Evolution: Is There a Tradeoff of Hydraulic Efficiency for Vulnerability to Dysfunction?" *IAWA Journal* 15, no. 4: 335–360.

Urli, M., A. J. Porté, H. Cochard, Y. Guengant, R. Burlett, and S. Delzon. 2013. "Xylem Embolism Threshold for Catastrophic Hydraulic Failure in Angiosperm Trees." *Tree Physiology* 33, no. 7: 672–683. https://doi.org/10.1093/treephys/tpt030.

Venturas, M. D., F. D. Rodriguez-Zaccaro, M. I. Percolla, C. J. Crous, A. L. Jacobsen, and R. B. Pratt. 2016. "Single Vessel Air Injection Estimates of Xylem Resistance to Cavitation Are Affected by Vessel Network Characteristics and Sample Length." *Tree Physiology* 36, no. 10: 1247–1259. https://doi.org/10.1093/treephys/tpw055.

Virtanen, P., R. Gommers, T. E. Oliphant, et al. 2020. "SciPy 1.0: Fundamental Algorithms for Scientific Computing in Python." *Nature Methods* 17, no. 3: 261–272. https://doi.org/10.1038/s41592-019-0686-2.

Vite, J. P., and J. A. Rudinsky. 1959. "The Water Conducting Systems in Conifers and Their Importance in the Distribution of Trunk-Injected Chemicals." *Contributions. Boyce Thompson Institute for Plant Research* 20, no. 1: 27–38.

Wagner, Y., F. Feng, D. Yakir, T. Klein, and U. Hochberg. 2022. "In Situ, Direct Observation of Seasonal Embolism Dynamics in Aleppo Pine Trees Growing on the Dry Edge of Their Distribution." *New Phytologist* 235, no. 4: 1344–1350. https://doi.org/10.1111/nph.18208.

Wagner, Y., M. Volkov, D. Nadal-Sala, N. K. Ruehr, U. Hochberg, and T. Klein. 2023. "Relationships Between Xylem Embolism and Tree Functioning During Drought, Recovery, and Recurring Drought in Aleppo Pine." *Physiologia Plantarum* 175, no. 5: e13995. https://doi.org/10.1111/ppl.13995.

Waisel, Y., N. Liphschitz, and Z. Kuller. 1972. "Patterns of Water Movement in Trees and Shrubs." *Ecology* 53, no. 3: 520–523. https://doi.org/10.2307/1934244.

Zanne, A. E., K. Sweeney, M. Sharma, and C. M. Orians. 2006. "Patterns and Consequences of Differential Vascular Sectoriality in 18 Temperate Tree and Shrub Species." *Ecology* 20, no. 2: 200–206.

Ziemińska, K. 2023. "The Role of Imperforate Tracheary Elements and Narrow Vessels in Wood Capacitance of Angiosperm Trees." *IAWA Journal* 7, no. 1: 1–14. https://doi.org/10.1163/22941932-bja10116.

Supporting Information

Additional supporting information can be found online in the Supporting Information section. **Figure S1:** Stem cross sections of two di erent oak seedlings (A–H, respectively) showing the emergence of leaf traces. Stems were manually cross sectioned starting at 2 mm below the leaf node (A, E) up to the leaf node (D, H) with intermediate points (B, C, F, G). Black arrows indicate the leaf trace. Scale bar is 1 mm. **Figure S2:** Cross sections of uCT scans of one example notched oak stem showing the emergence of a leaf trace directly above the notch. Iohexol solution was fed to the stem as a contrast agent. Areas containing Iohexol appear brighter. Cross sections are from di erent heights starting at 1 mm below the leaf node (A) up to the leaf node (F). Orange circles indicate the partly embolized vessels of the leaf trace. Scale bars are 1 mm.